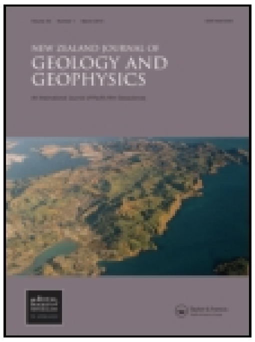

Taylor & Francis
Taylor & Francis Group

New Zealand Journal of Geology and Geophysics

ISSN: 0028-8306 (Print) 1175-8791 (Online) Journal homepage: http://www.tandfonline.com/loi/tnzg20

A revision of mid-late Holocene marine terrace distribution and chronology at the Pakarae River mouth, North Island, New Zealand

Kate Wilson , Kelvin Berryman , Nicola Litchfield & Tim Little

To cite this article: Kate Wilson , Kelvin Berryman , Nicola Litchfield & Tim Little (2006) A revision of mid-late Holocene marine terrace distribution and chronology at the Pakarae River mouth, North Island, New Zealand, New Zealand Journal of Geology and Geophysics, 49:4, 477-489, DOI: 10.1080/00288306.2006.9515182

To link to this article: http://dx.doi.org/10.1080/00288306.2006.9515182

Published online: 22 Sep 2010.

New Zealand Journal of Geology & Geophysics, 2006, Vol. 49: 477–489 477
0028–8306/06/4904–0477

A revision of mid–late Holocene marine terrace distribution and chronology at the Pakarae River mouth, North Island, New Zealand

KATE WILSON[1*]
KELVIN BERRYMAN[2]
NICOLA LITCHFIELD[2]
TIM LITTLE[1]
[1]School of Earth Sciences
Victoria University of Wellington
PO Box 600
Wellington 6140, New Zealand
[2]GNS Science
PO Box 30368
Lower Hutt 5040, New Zealand
[*]Present address: GNS Science, PO Box 30368, Lower Hutt 5040, New Zealand.

Abstract A suite of seven marine terraces at the Pakarae River mouth, New Zealand, provide evidence for the highest Holocene coastal uplift rates adjacent to the Hikurangi Subduction Zone. New elevation, coverbed stratigraphy, and age data allow for a timely revision of the distribution, nomenclature, and chronology of these terraces. Terrace correlation primarily is based on the elevation of the wave-cut strath. Terrace preservation either side of the river is more equal than previously proposed. The age of abandonment of each terrace is c. 7 ka (T1), 4.3 ka (T2), 3.5 ka (T3), 2.89 ka (T4), 1.6 ka (T5), 0.91 ka (T6), and <0.91 ka (T7). The average Holocene tectonic uplift rate at Pakarae is 3.2 ± 0.8 mm/yr. The abandonment of each terrace, from T2 to T7, probably took place after a discrete uplift event. The average time interval between these events is 850 ± 450 yr and the average uplift magnitude is 2.7 ± 1.1 m per event. We infer that uplift has been accommodated by slip on an offshore reverse fault. Normal slip on the Pakarae Fault, at right angles to the margin, occurs at a comparatively slower rate and has probably made little contribution to coastal uplift.

Keywords marine terraces; Pakarae River; coastal uplift; neotectonics

INTRODUCTION

The Pakarae River mouth locality (henceforth called Pakarae) has the greatest number of Holocene marine terraces of any location adjacent to the Hikurangi Subduction Zone (Berryman et al. 1989; Ota et al. 1991, 1992). Seven terraces elevated above modern mean sea level (MSL) provide evidence of past sudden coastal uplift since sea level (SL) stabilised in the mid Holocene. The well-preserved record of coastal uplift distinguishes the Pakarae location as one of the most tectonically active coastal areas of the Pacific Rim (Berryman et al. 1992; Ota & Yamaguchi 2004). Accurate knowledge of the timing, frequency, and magnitude of coastal uplift for each event at Pakarae provides a long record of tectonism in the subduction margin. The proximity of the study location to a subduction thrust (that has no historic record of slip during large or great earthquakes), and a normal fault offsetting the terraces locally at Pakarae, begs the question of what fault, or faults, is driving the rapid coastal uplift rates along this part of the Hikurangi margin.

Moderate to high late Quaternary coastal uplift rates (0.5–3 mm/yr) have been recorded by marine terraces at many locations along the Raukumara Peninsula (Fig. 1A–D); the Pakarae region has the highest Holocene uplift rates recorded along this segment of the Hikurangi margin (Ota et al. 1988, 1992; Yoshikawa 1988; Berryman et al. 1989; Berryman 1993). Offshore of Pakarae, directly to the east, is the Hikurangi Subduction Zone (Fig. 1A); the continental shelf has been deformed by strike slip, contractional, and extensional faulting, and several margin indentations may indicate previous seamount collisions (Collot et al. 1996). In the vicinity of Pakarae, Oligocene and Miocene marine siltstones and mudstones are juxtaposed across the Pakarae Fault, a north-striking structure on the western side of the Pakarae River (Kingma 1964; Mazengarb & Speden 2000). Several short segments of active normal faults have been mapped in the Pakarae region, including the Pakarae Fault (Fig. 1D) and the Waihau Bay Fault, located 10 km north of Pakarae (Mazengarb 1984, 1998; Mazengarb & Speden 2000). Walcott (1987) and Thornley (1996) inferred that the Raukumara Peninsula is undergoing margin-normal extension due to uplift driven by sediment underplating. The character of active faulting at Pakarae is therefore of relevance to understanding the geodynamic relationships between onshore normal faults, offshore upper plate compressional structures, and the subduction interface.

The Pakarae Holocene marine terraces were previously mapped, correlated, and dated by Ota et al. (1991). Seven terraces, named T1–T7, from oldest to youngest, were recognised at Pakarae. T1 corresponds to the maximum mid-Holocene marine transgression at c. 7 ka (Gibb 1986). The terraces were correlated across the Pakarae River based on their age and height. Only terraces T4 and T5 were mapped on both sides of the river. Landward tilting of the terraces was indicated by terrace height projections normal to the coast (Ota et al. 1991). The timing of uplift of each terrace was estimated from tephra coverbed distribution and radiocarbon ages of shells that were collected from close to the wave-cut strath. Shells from T1–T6 were collected for radiocarbon dating either from natural river bank exposures of the marine terrace coverbeds on the west bank, or from soil pits excavated on the eastern bank. T7 was dated by correlation to the lowest terrace at Waihau Bay, 15 km north of Pakarae, which is overlain by sea-rafted Loisells Pumice. Originally thought to be uniformly <700 yr BP (McFadgen 1985), this pumice is

G06007; Online publication date 22 November 2006
Received 15 March 2006; accepted 18 October 2006

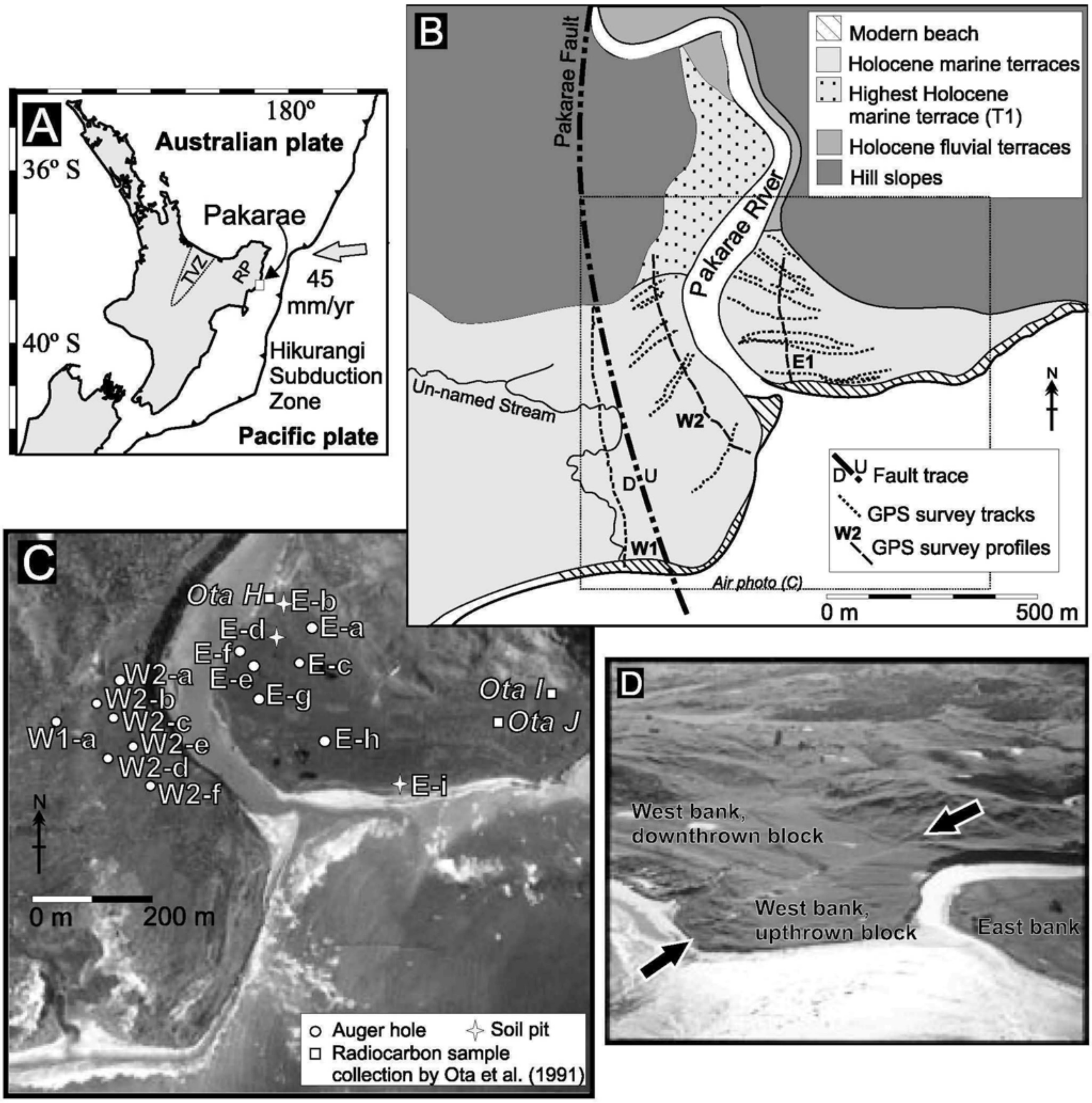

Fig. 1 The Pakarae River mouth locality. **A**, Location map and the Hikurangi Subduction Zone, North Island New Zealand. RP, Raukumara Peninsula; TVZ, Taupo Volcanic Zone. Arrow shows the relative plate motion vector from De Mets et al. (1994). **B**, Major geomorphic features of the Pakarae River mouth and GPS survey lines referred to in text. W1, W2 and E1 refer to elevation profiles shown in Fig. 2. **C**, Locations of cover sediment profiles shown in Fig. 2. Points "Ota ..." are radiocarbon date collection locations of Ota et al. (1991) referred to in text. **D**, Oblique aerial photo of the Pakarae River mouth showing the geomorphology of the Pakarae Fault (arrowed).

now acknowledged to be diachronous in its age at different sites around the New Zealand coastline (Shane et al. 1998).

As part of a broader study at Pakarae we have collected new information on terrace elevation, coverbed stratigraphy, including tephra, and ages of fossils in the terrace deposits. These new data provide the basis for revising the correlation of the terraces across the Pakarae River and for reconsidering the timing and rates of Holocene coastal uplift events. In this study we use 3 GPS elevation profiles across the terraces, 16 terrace cover sediment profiles, and 3 new radiocarbon ages to revise the original terrace distribution and chronology detailed by Ota et al. (1991). The geomorphology and age of the raised terraces allow inferences to be made regarding the types of faults most likely to have played a key role in the uplift of this coast.

METHODS

In this study we use the following terminology: **marine terraces** refer to relict coastal erosion surfaces overlain by marine and non-marine cover sediments; risers separate the

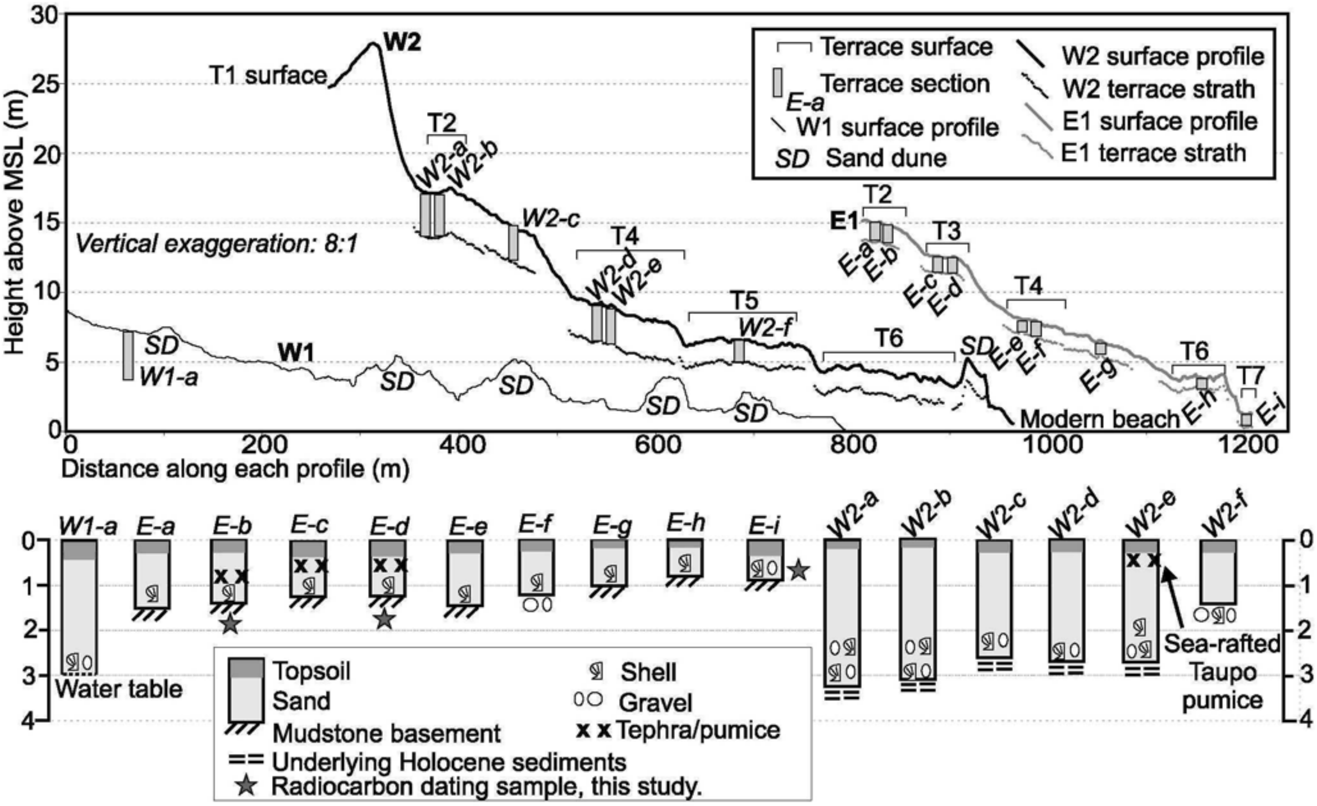

Fig. 2 **(Top)** GPS height profiles across the Pakarae Holocene marine terraces, location of profiles shown on Fig. 1. Profiles W2 and E1 have the terrace straths plotted based on the amount of cover material on each terrace; location of the soil pits and auger holes shown. Profile E2 not shown as it is similar to E1. See text for discussion of the GPS elevation uncertainties. **(Below)** Simplified coverbed stratigraphy on the Holocene marine terraces from soil pits and augering.

terraces. **Wave-cut strath** refers to the surface cut by coastal erosion processes when the surface was approximately at MSL; the **shoreline angle** is the angle formed at the landward edge of a terrace where strath intersects the riser to the higher terrace; the **terrace surface** refers to the modern surface of the terrace, which includes a certain thickness of cover sediments deposited since the sea abandoned the terrace.

A microtopographic survey of the terrace surfaces was carried out using a Real Time Kinematic (RTK) GPS. The elevations have an uncertainty of ±0.16 m at a 95% confidence interval. The perimeter of each terrace on the east bank and on the upthrown side of the fault on the west bank was surveyed. Linear profiles across all terraces were also made: W1 on the west bank on the downthrown side of the fault, and W2 on the west bank, upthrown side of the fault, and E1 on the east bank (Fig. 1B).

The stratigraphy of the terrace sediment cover was determined at 16 locations using a hand auger or soil pits (Fig. 1C). Coverbed sediments were described by a visual assessment of their colour and grain size (Fig. 2).

Our height correlations between the terraces are based on the elevation of the wave-cut straths, which we obtained by subtracting the depth of cover sediment from the terrace surface elevation, as determined from the GPS. On approximately one-half of the terraces we had two measurements of the cover sediment thickness over the wave-cut strath and there was always <0.15 m difference between the two measurements (the av. difference was 0.1 m, Fig. 2). Given that 0.1 m is less than the elevation measurement uncertainty on each terrace, it was not deemed essential to take more than one measurement of cover sediment thickness per terrace. However, we assign a 95% uncertainty of ±0.5 m to the elevations of the wave-cut straths to take account of irregularities created by variable erosion of the platforms. To calculate the elevation of the wave-cut strath of the lowest terrace on the west bank we used the cover sediment thickness from the terrace above it as an approximate measure of the cover sediment thickness (Fig. 2); this assumption may result in a slight underestimation of the wave-cut strath elevation as there is a trend of decreasing cover sediment thickness with decreasing age. Therefore, the lowest terrace probably has slightly less cover sediment than the one above it. Only one auger hole was taken on the downthrown side of the fault: this sampled the highest terrace. The auger hole reached the water table at 3 m and further sediment recovery was not possible. With the surface elevation of the terraces having an uncertainty of ±0.16 m and the cover sediment thickness variation <0.15 m, we believe ±0.5 m is a conservative estimate of the uncertainty at a 95% confidence interval for the elevation of each of the wave-cut straths at the Pakarae River mouth.

Shell material was collected for radiocarbon dating from all auger holes and soil pits (Fig. 2, 3). We always collected shells from as close as possible to the wave-cut strath. These shells occur within coarse sand and mudstone-clast gravels that represent the paleo-beach deposits at the time when the terrace was being cut. Whole shells were collected if present,

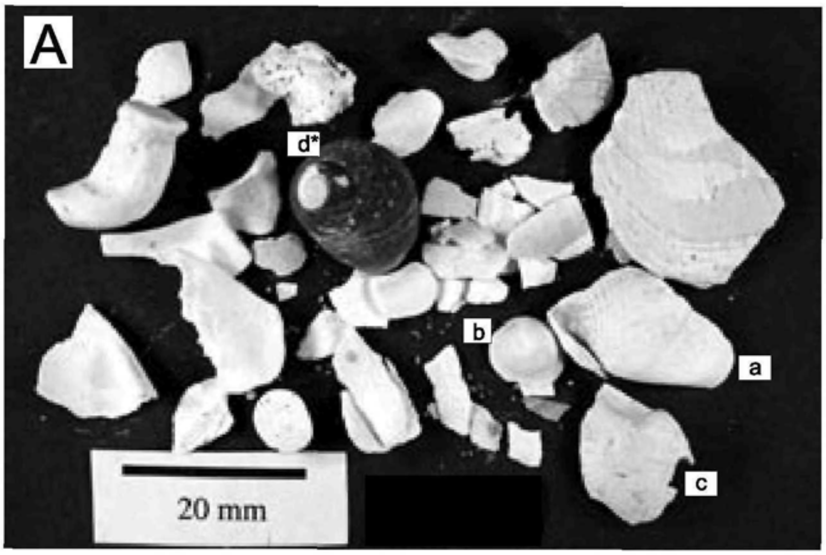

Scale bar: centimetres

Fig. 3 Shell species and radiocarbon samples from the Pakarae marine terraces. * radiocarbon AMS sample. **A**, T2 north bank: (a) fragment of *Pholadidea* spp., (b) fragments of cat's eye (Ataota), *Turbo smaragdus*, (c) fragments of cockle, *Austrovenus stutchburyi*, (d) spotted top shell (Maihi), *Melagraphia aethiops* and unidentified shell fragments. **B**, T6 north bank: (a) scimitar shell (Peraro) *Zenatia acinaces*, (b) fragments of cat's eye (Ataota), *Turbo smaragdus* and unidentified shell fragments. **C**, T3 north bank: (a) blue mussel (Toretore), *Mytilus edulis galloprovincialis*, (b) fragments of cat's eye (Ataota), *Turbo smaragdus*, (c) fragments of cockle, *Austrovenus stutchburyi*, (d) spotted top shell (Maihi), *Melagraphia aethiops* and unidentified shell fragments.

otherwise well-preserved shell fragments were collected; the shell species have been identified where possible (Fig. 3). Accelerator mass spectrometer (AMS) radiocarbon ages of shells were determined at the Rafter Radiocarbon Laboratory, Institute of Geological & Nuclear Sciences Ltd. We chose to date only terraces which had the highest age uncertainty as most of the terraces have been previously dated by Ota et al. (1991). The radiocarbon ages of Ota et al. (1991) have been calibrated for use in this study using the marine calibrations of Hughen et al. (2004). All radiocarbon ages will be presented as the 2 σ age estimate in calibrated years before present (cal. yr BP). Tephra was identified by its physical characteristics, age relationships, and comparison with tephra isopach maps of Vucetich & Pullar (1964).

RESULTS

Marine terrace characterisation

RTK GPS profiles oriented approximately normal to the terraces show distinctive staircase topography with flat to gently sloping surfaces separated by steep risers (Fig. 2). The terrace surfaces are up to 120 m wide and display morphology similar to the modern beach mudstone platform, which is exposed from the beach out to c. 150 m offshore within the intertidal surf zone. From terrace profiles W2 and E1 we can identify six terraces on the west bank and six terraces on the east bank of the Pakarae River. On the downthrown side of the Pakarae Fault (profile W1), separate terraces were not differentiated because they are covered by sand dunes (Fig. 2). Therefore, discussions of the west bank terraces refer to the upthrown side of the fault only.

Cover sediment thickness is greatest on the west bank, while on both sides of the river there is a general decrease in cover sediment thickness with decreasing terrace elevation, possibly reflecting a greater accumulation of aeolian sand over time (Fig. 2). Cover sediment stratigraphy generally fines upwards. The basal deposits sit directly on the wave-cut strath and are everywhere coarse sand with shells (whole shells, and shell hash) and mudstone-clast gravel (Fig. 2). On the east bank all wave-cut straths are incised in mudstone. On the west bank all wave-cut straths, except underlying the most recent two terraces, are incised into hard, mottled fluvial silts (Fig. 2). These silts were deposited by the Pakarae River during the early Holocene when the coastline was farther to the east. Shell species in the beach deposits (Fig. 3) are mostly from rocky shore habitats and all are from intertidal environments (Morton & Miller 1968; Marsden & Pilkington 1995; Marsden 2004; Morton 2004). The beach deposits are overlain by well-sorted, massive medium sand barren of shells. The change from coarse shelly sand to medium unfossiliferous sand represents a transition between shoreface beach sands and aeolian sands. Dark brown topsoil has developed on the aeolian sand on all terraces.

The depths of cover sediment that we measured on the east bank are similar to those of Ota et al. (1991). Both studies included the use of soil pits to measure sediment thickness above the wave-cut strath. On the west bank our measurements of cover sediment thickness are significantly less than those of Ota et al. (1991) (cf. second highest terrace: our study, 3.2 m; Ota et al. 1991, 5 m). The difference is because we obtained sediment thickness in the middle of the terrace surface, whereas Ota et al. (1991) used outcrops along the riverbank. Our recent observations along the riverbank reveal that much of it has slumped and therefore these outcrops overestimate the thickness of sediment and underestimate the elevation of the wave-cut strath.

Terrace ages

Three new shell radiocarbon ages from the east bank were obtained: from the highest (14 m), second highest (11.5 m), and the lowest (1 m) terraces (Fig. 2, Table 1). The two highest terraces on the east bank have a mantle of Waimihia Tephra (3430–3470 cal. yr BP; Froggatt & Lowe 1990). The Waimihia Tephra is identified by its age relationship to the highest terrace (i.e., must be <c. 7 ± 0.5 ka BP, the time of eustatic SL stabilisation; Gibb 1986) and its coarse lapilli texture. The middle terrace of the west bank has a layer of sea-rafted pumice clasts within the sand (section W2-c). We identify this as the Taupo Pumice based on its age relationships to the terraces and other known occurrences of this pumice along the east coast of the North Island. These rounded pumice clasts are up to 5 cm in diameter; they are probably a storm-deposit and indicate that the terrace is older than the age of the Taupo eruption at 1720–1600 cal. yr BP (Froggatt & Lowe 1990).

DISCUSSION

Terrace correlation and chronology

Revised terrace correlations across the Pakarae River are primarily based on new data on the elevation of the shoreline angles and wave-cut straths, and we also use two of the three additional radiocarbon ages (Table 1). We consider that the elevation of the shoreline angle is the most reliable feature for correlating the terraces because this would have been the same on both sides of the river.

One potential problem with correlating shoreline angle elevations across the river is the possible influence of tilting due to movement on the Pakarae or other faults. Projections of the terrace surface elevations to an east–west plane striking approximately normal to the Pakarae Fault show a small gradient (0.19°, 3.4 m/km) of terrace tilt towards the west (Fig. 4A), a gradient not significant enough to affect terrace correlations across the c. 100 m wide Pakarae River. Ota et al. (1991) also documented westward tilt normal to the Pakarae Fault. However, they interpreted this as evidence of landward tilt. We confirm landward tilt by projecting the terrace surface elevations to a plane striking normal to the Pakarae River and approximately normal to the Hikurangi subduction margin (Fig. 4). The projected elevations show a 0.23° landward tilt (a gradient of 4.1 m/km, Fig. 4).

Our terrace correlations indicate the presence of seven distinct terraces (Fig. 5). This is the same number as determined by Ota et al. (1991); however, our terrace distribution and correlation is significantly different (cf. Fig. 5B,C). In several cases there are conflicting radiocarbon ages from what are interpreted to be the same terrace. We resolve this by recognising that tephra occurrence provides an age constraint that can help distinguish which radiocarbon ages are more likely to be correct. We then consider from where the radiocarbon samples were collected. Some samples collected by Ota et al. (1991) are from areas where the terraces are indistinct and difficult to map and correlate. Lastly, we give preference to younger radiocarbon ages. We cannot see a mechanism for transporting young shell into the basal beach deposits of higher terraces, yet there are several mechanisms by which older shells could be recycled onto lower terraces. The following details the nomenclature, correlation, and distribution of each terrace from oldest (T1) to youngest (T7):

T1: The T1 surface is present only on the west bank (Fig. 5B,C). Our interpretation agrees with Ota et al. (1991) that this is the maximum Holocene SL transgression surface of c. 7 ± 500 cal. yr BP (we estimate a 95% uncertainty of 500 yr for the timing of eustatic SL stabilisation based on Gibb 1986). The oldest marine sediments underlying this surface have been dated at 7430–7280 cal. yr BP by Wilson et al. (in press), therefore constraining the timing of uplift to younger than 7430–7280 cal. yr BP.

T2: T2 is the second highest terrace on the west bank and the highest terrace on the east bank (Fig. 5C). It was previously

Table 1 Radiocarbon age data collected during this study from the Pakarae marine terraces.

Sample height (m)	Sample name	Sample material	Dating technique	^{13}C (‰)	Radiocarbon age* (radiocarbon yr BP)	Calibrated age† 2 σ (cal. yr BP)	Lab. number‡
14	East highest terrace	Shell, *Melagraphia aethiops*	AMS	1.33	4148 ± 30	4391–4138	NZA 22657
11.5	East 2nd highest terrace	Shell, *Mytilus edulis galloprovincialis*	AMS	0.52	3582 ± 30	3610–3403	NZA 22659
1	East lowest terrace	Shell, *Zenatia acinaces*	AMS	–8.48	2078 ± 30	1802–1582	NZA 22658

*Conventional radiocarbon age before present (AD1950) after Stuiver & Polach (1977).
†Marine□
‡NZA: Institute of Geological & Nuclear Sciences Rafter Radiocarbon Laboratory.

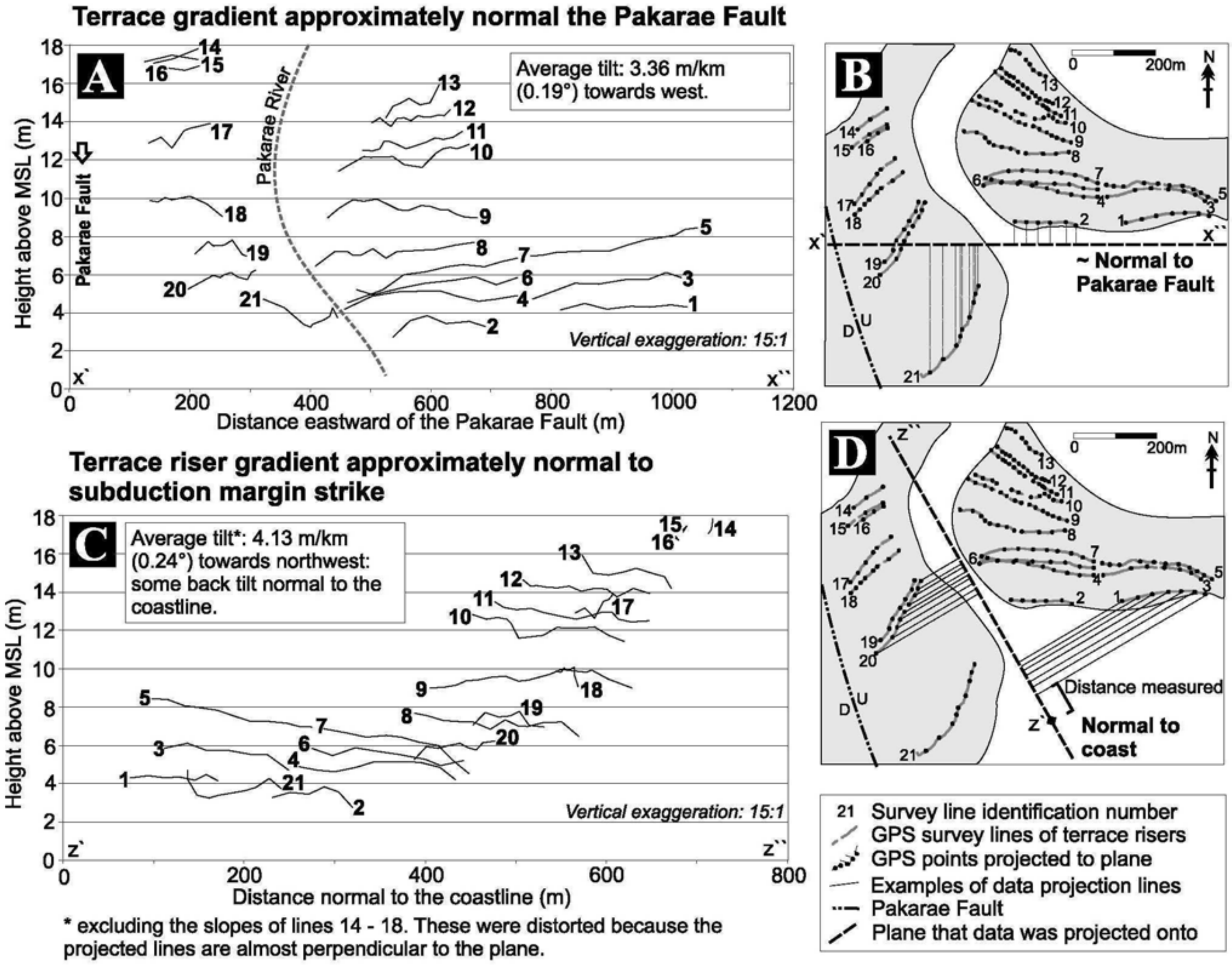

Fig. 4 Height profiles along the Pakarae terrace risers. Riser heights are projected to a plane approximately normal to the Pakarae Fault (A,B) and to a plane approximately normal to the Hikurangi subduction margin (C,D). The profiles test whether the terraces are back tilted relative to the Pakarae Fault or the subduction margin.

mapped as T3 on the east bank by Ota et al. (1991) because it had a younger radiocarbon age than the terrace of similar elevation on the west bank terrace (6410–6138 cal. yr BP on the west bank versus 4602–4130 cal. yr BP on the east bank; Ota et al. 1991). Our radiocarbon age of this terrace of 4391–4138 cal. yr BP on the west bank supports a younger terrace age of c. 4300 cal. yr BP, which is also consistent with the presence of the Waimihia Tephra in the terrace cover sediments. We therefore revise the terrace correlation in spite of the age difference inferred by Ota et al. (1991) because the shoreline angles are almost identical in elevation (c. 14 m AMSL) on both sides of the river. We interpret the older (c. 6.3 ka) radiocarbon age obtained by Ota et al. (1991) from the west bank as a reworked shell.

T3: The T3 terrace is the second highest terrace on the east bank but is less distinct on the west bank (Fig. 2). On the west bank, T3 has a significant surface gradient; however, this gradient is considerably less than that of the other risers, and we infer it to be a modified terrace surface. In the field, the T3 terrace on the west bank is sufficiently clear that its perimeter could be mapped. The seaward edge of the slope of the wave-cut strath on the west bank is the same elevation as the wave-cut strath of T3 on the east bank. The steeper terrace slope observed on the west bank T3 may result from poor wave-cut strath planation or is more likely due to aeolian sand accumulation towards the rear of the terrace, which would also explain why there is no riser separating T2 and T3 on the west bank. On the east bank, T3 is mantled by the Waimihia Tephra (3430–3470 cal. yr BP), and we obtained a radiocarbon age of 3610–3403 cal. yr BP from beneath the tephra; an age of 2714–2338 cal. yr BP was obtained by Ota et al. (1991). We prefer our radiocarbon age as an estimate of the age of the second highest terrace because it is compatible with the presence of the overlying 3430–3470 cal. yr BP Waimihia Tephra. Furthermore, the location of Ota et al.'s sample yielding the 2714–2338 cal. yr BP age is farther away from the river mouth at a location where terrace risers become less distinctive. For this reason, we could not map the terrace distribution in the eastern area (Fig. 5C), and it is possible the young age of Ota et al. (1991) is not from a terrace correlative to the second highest terrace as defined by us close to the river. Ota et al. (1991) previously mapped T3 only on the east bank, where it was their highest terrace (Fig. 5B). We revise this in light of our new age estimates of the terrace and our data on the wave-cut strath elevations (Fig. 5C).

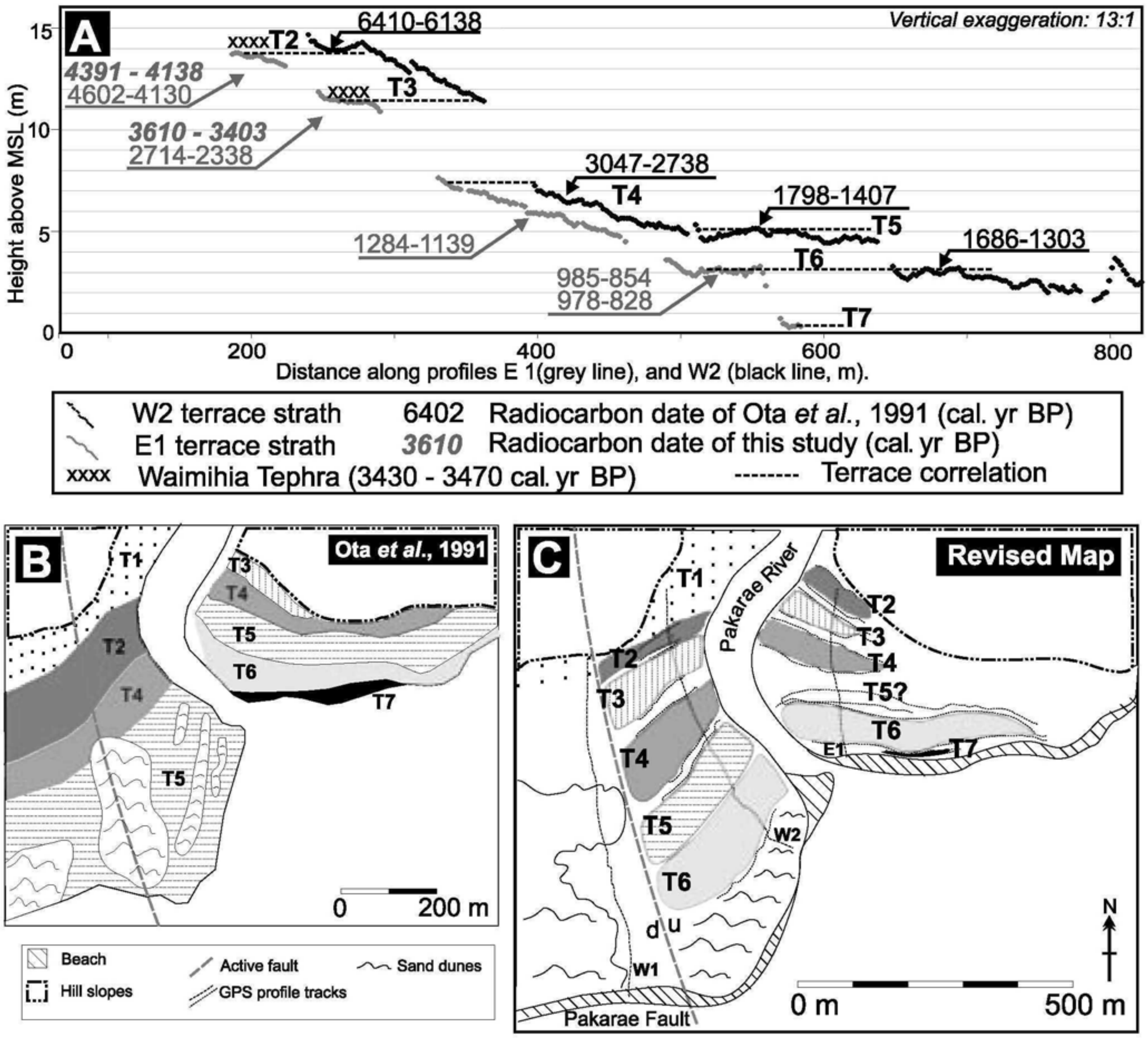

Fig. 5 **A**, Profiles showing wave-cut surface elevation with radiocarbon dates and surface correlation between the east and west banks of the Pakarae River. **B**, Marine terrace distribution at Pakarae; original map by Ota et al. (1991). **C**, Revised terrace distribution of this study.

T4: The T4 terrace is the middle terrace on both banks. Our mapping agrees with Ota et al. (1991) on the west bank but not on the east bank where they called it T5 (Fig. 5B,C). We found scattered sea-rafted Taupo Pumice clasts on this terrace on the west bank, as did Ota et al. (1991). They also found the same clasts on what we are calling T4 on the east bank, but despite this they mapped it as T5 on the east side. The mapping of these as different terraces by Ota et al. (1991) is plausible given that the sea-rafted pumice can be of diachronous age and deposited by storm waves some distance from the shoreface, but the simplest interpretation in our view is that these terraces are the same age. The terrace surface of T4 is relatively wide and gently sloping with the shoreline angles at 7.5 m AMSL and mid points of the wave-cut strath at c. 6 m AMSL on both banks. Another distinctive feature common to the T4 terrace on both sides of the river is that the riser on the landward side of the terrace is particularly high: 4 m compared to typical 2–2.5 m riser heights for other terraces (Fig. 2). Ota et al. (1991) obtained a radiocarbon date of 3047–2738 cal. yr BP from this terrace on the west bank and 1284–1139 cal. yr BP on the east bank. The presence of Taupo Pumice (erupted 1720–1600 cal. yr BP; Froggatt & Lowe 1990) as a storm beach deposit constrains the terrace age to the older date because pumice would not occur as part of the basal beach deposit if the younger age were correct. The east bank radiocarbon sample was collected from a location far to the east of the river mouth (point "Ota-J", Fig. 1C), where the terraces are indistinct, and therefore this sample may date a terrace younger than T3. For these reasons we prefer to use the older radiocarbon age of 3047–2738 cal. yr BP as the age of this terrace.

T5: The T5 terrace is distinctive on the west bank but poorly developed or preserved on the east bank (Fig. 2, 5). On the west bank, T5 is wide and gently sloping with sharp 1–2 m risers above and below. Ota et al. (1991) also mapped this surface as T5 (Fig. 5B); however, their T5 is wider than our definition of T5 (Fig. 5C). The narrowing of T5 between interpretations is because we have subdivided Ota et al.'s T5 into T5 and T6 terraces. Both our profiles and that of Ota et al. (1991) show a step in the surface topography of c. 1.5 m at our T5/T6 riser; however, Ota et al. (1991) did not split the terrace here apparently because the lower section yielded a similar radiocarbon date to the upper one (1783–1418 cal. yr BP upper strath, 1680–1307 cal. yr BP lower strath). We do not have any auger holes from the lower surface to verify that there is a step down in the wave-cut strath elevation, but the surface topography is clearly stepped and therefore we have divided the terrace into two. The radiocarbon date of Ota et al. (1991) from the lower strath may have been derived from a reworked shell. On the east bank, the profile of E1 between T4 and T6 is gently sloping with only a small riser at the front edge of T4. We do not map a terrace in here because the morphological expression is indistinct; however, the wide horizontal spacing between T4 and T6 suggests that time may have elapsed between the formation of these terraces. We therefore suggest that T5 is also present on the east bank where it was either weakly developed or has been poorly preserved as a result of aeolian deposition or riser scarp erosion. We retain the age of 1798–1407 cal. yr BP collected by Ota et al. (1991) for this terrace.

T6: As discussed above, we have reasonable evidence from surface morphology for an additional terrace on the west bank that we call T6 (Fig. 5C). On the east bank, our T6 is equivalent to that of Ota et al. (1991) (Fig. 5B). Two radiocarbon samples obtained by Ota et al. (1991) from the east bank, close to the river mouth, date the terrace at 985–854 and 978–828 cal. yr BP.

T7: T7 occurs as a thin strip on the east bank. Our mapping of this terrace agrees with that of Ota et al. (1991) (Fig. 5B,C). The age of this terrace was previously estimated by correlation to a terrace 15 km north along the coast, which has the Loisells Pumice on it. The Loisells Pumice is no longer thought to be everywhere <600 yr BP (Shane et al. 1998), so the age assigned to T7 needs to be reconsidered. We obtained a shell sample from the mudstone platform and it was radiocarbon dated at 1802–1582 cal. yr BP (Fig. 3, Table 1). Given the ages of 985–854 and 978–828 cal. yr BP for T6, we suspect that our shell sample was reworked. It is possible that T7 is also present on the west bank, however dune sands probably bury it (Fig. 2).

Tectonic uplift rates

We agree with Ota et al. (1991) that each terrace was formed by a sudden uplift event that caused the abandonment of the wave-cut surface by the sea (see Ota et al. 1991 for discussion). The New Zealand Holocene eustatic SL curve shows that, since the c. 7 ka culmination, SL has remained near its modern position with only minor fluctuations of the order of <0.5 m (Gibb 1986). We can therefore assume that the present elevation of each terrace above modern mean SL is due almost entirely to tectonic uplift. The likeness of the terrace coverbed sands and constituent shell species to the modern beach intertidal sand and shell accumulations supports the inference that the terraces were formed by coastal processes similar to those operating on the modern beach. We also agree with Ota et al. (1991) that radiocarbon ages of shells from the wave-cut strath are likely to be (at least) slightly older than

Table 2 Age-elevation relationships between the Pakarae River marine terraces including average uplift rates.

Terrace	Elevation of shoreline angle (±0.5 m)	Height difference between terraces (±1 m)	Estimated age (cal. ka BP)	Uncertainty*	Time since previous events (ka)	Uncertainty§	Uplift rate (wave-cut strath elevation /estimated age: m/ka)	Uncertainty†
T1	24		7[a]	±0.5			3.4	±0.2
T2	13.8	10.2‡	4.3[b]	±0.2	na[g]	±0.4	3.2	±0.2
T3	11.5	2.3	3.5[c]	±0.1	0.8	±0.3	3.3	±0.2
T4	7.5	4	2.9[d]	±0.2	0.6	±0.2	2.6	±0.2
T5	5.0	2.5	1.6[e]	±0.2	1.3	±0.3	3.13	±0.5
T6	3.0	2	0.9[f]	±0.1	0.7	±0.2	3.3	±0.6
T7	0.5	2.5	–		–		–	
Average		2.7† ± 1.1¶			0.85†	±0.45¶	3.2	±0.8¶

*This uncertainty assumes a normal distribution of ages around the mean, however this is not true for the calibrated ages, but we assume this for simplification.
†Calculations do not include difference between T1 and T2.
‡Height may reflect erosion of missing terraces between T1 and T2.
¶Uncertainty = $\sqrt{[(\text{error}^2) + (\text{error}^2) + \ldots]}$.
§Uncertainty = $\sqrt{[(\%\ \text{elevation error})^2 + (\%\ \text{age error})^2]}$.
[a]Aged based on the timing of eustatic SL stabilisation after Gibb (1986); estimated uncertainty of ±500 yr.
[b]Radiocarbon dates from T2, this study and Ota et al. (1991): (4391+4138+4602+4130)/4; uncertainty is the larger half difference between the 2 σ calibrated age of the two samples.
[c]Mid point 3610–3403 cal. yr BP, this study; uncertainty is half the difference between the 2 σ calibrated ages.
[d]Mid point 3047–2738 cal. yr BP, Ota et al. (1991); uncertainty is half the difference between the 2 σ calibrated ages.
[e]Mid point 1798–1407 cal. yr BP, Ota et al. (1991); uncertainty is half the difference between the 2 σ calibrated ages.
[f]Radiocarbon ages from T6, Ota et al. (1991): (985+854+978+828)/4; uncertainty is the larger half difference between the 2 σ calibrated age of the two samples.
[g]Not applicable as there have probably been terraces eroded between T1 and T2.

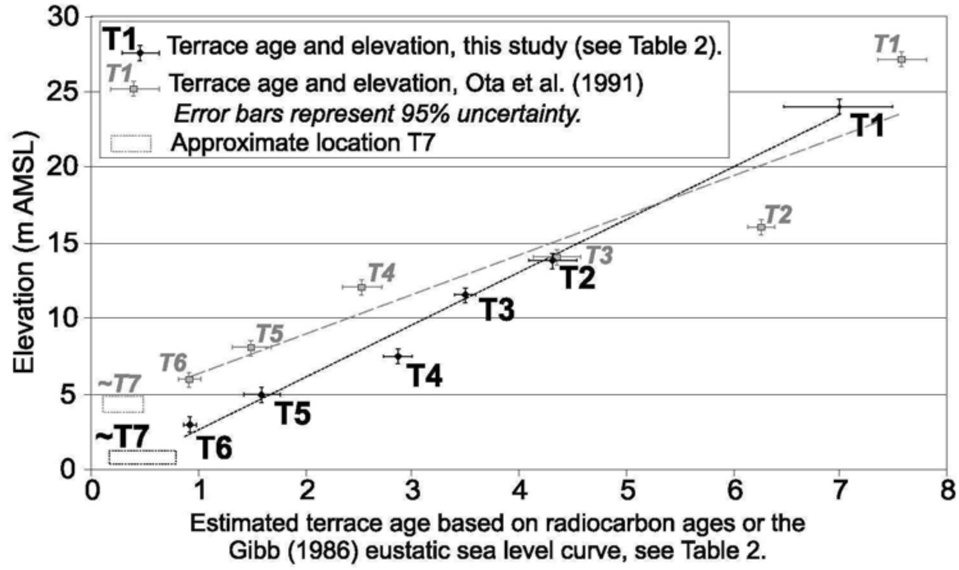

Fig. 6 Estimated terrace age (see Table 2) versus elevation. The ages of Ota et al. (1991) were calibrated (Hughen et al. 2004); the value shown here is the mid-point of the 2 σ calibrated age.

the timing of uplift and their abandonment—assuming that uplift caused the death of the organism. The well-preserved nature of the dated samples suggest there has been very little, if any, reworking the samples (Fig. 3). We use these ages to approximate a maximum limit for the time since uplift.

Our revised terrace ages are summarised in Table 2. On the modern beach the mudstone platform is being cut at approximately the mid-tide level, therefore we assume the uplifted wave-cut strath, measured at the shoreline angle, approximately represents mean SL prior to terrace uplift. The elevation difference between the wave-cut strath and modern mean SL equals the tectonic uplift. The mean uplift rates appear to have been remarkably uniform since c. 7 ka. We calculate an average rate of 3.2 ± 0.8 mm/yr (Fig. 6, Table 2). From T2 to T7 each terrace probably represents one uplift event; the average time interval between events is 850 ± 450 yr and the average magnitude is 2.7 ± 1.1 m per event. These are maximum values; it is possible that terraces produced by smaller events have not been preserved. Discounting the elevation and time difference between T1 and T2, because we believe terraces have been eroded from this part of the terrace sequence, the terrace-forming uplift events at Pakarae have been more regular in terms of magnitude than previously thought (Fig. 6).

One major difference between our terrace distribution interpretation and that of Ota et al. (1991) is the age of our T2. Ota et al. (1991) assigned an age of 6410–6138 cal. yr BP to this terrace, whereas we revise this to c. 4300 cal. yr BP. Our age revision means there is more time between the formation of T1 and T2. The age assignment of Ota et al. (1991) has an age difference of 1670–830 yr between T1 and T2; this study has 3210–2170 yr. A greater age difference between T1 and T2 reconciles better with the very high riser height (10.2 m) between these two terraces. Between T1 and T2 we believe more than one uplift event occurred to account for the high terrace riser. It is unrealistic that a 10.2 m riser was created by a single event when the average riser height of all the younger terraces is c. 2.7 m. Terraces may have formed in the period between T1 and T2 (c. 7000–4300 cal. yr BP) but subsequently eroded.

Pakarae terrace uplift and the role of the Pakarae Fault

We seek to investigate the tectonic structures that have driven the coastal uplift at Pakarae. We can use the geomorphology and ages of the terraces and compare them with block models of how terraces would form under different faulting scenarios. The presence of a scarp of the Pakarae Fault across the <7 ka Pakarae terrace sequence is indisputable evidence that this fault has moved during the Holocene. However, the north–south strike of the fault and the presence of terraces on either side of the fault indicate it is not the sole cause of uplift of the marine terraces. Instead, we infer that the main cause of coastal uplift on both sides of the Pakarae Fault was slip on a westward-dipping offshore reverse fault (Fig. 7A,B). Other than the Pakarae Fault, the onshore region contains no other known active faults except for the Waihau Bay Fault, which is a normal fault located c. 15 km north of Pakarae. Fault scaling relationships imply that with the short surface trace of the Waihau Bay Fault, and its distance from Pakarae, it is unlikely this fault caused uplift at Pakarae.

Slip on the subduction interface is not a likely cause of uplift because preliminary dislocation modelling indicates an unrealistically large amount of slip on the subduction thrust is required to produce uplift of c. 2.7 m at Pakarae (Litchfield & Wilson 2005). Sixty kilometres SSW of Pakarae, the offshore Lachlan reverse fault, dipping 15–20° to the NW, has caused coseismic uplift of Holocene marine terraces c. 5 km westwards on the Mahia Peninsula (Berryman 1993; Barnes et al. 2002). Although no structure analogous to the Lachlan Fault has so far been seismically imaged offshore of Pakarae, we suggest a similar reverse fault may have caused coastal uplift at Pakarae (Fig. 7B). A reverse fault has been mapped offshore of Pakarae by Lewis et al. (1997) and Mazengarb & Speden (2000); however, this mapping was based on an estimated location by Ota et al. (1991). The fault location was estimated by Ota et al. (1991) based upon the distribution of Holocene marine terraces at the Pakarae River mouth and 15 km northeastward along the coastline.

Ota et al. (1991) also suggested that while the main fault driving the coastal uplift at Pakarae was a reverse fault located offshore, the Pakarae Fault also moved simultaneously

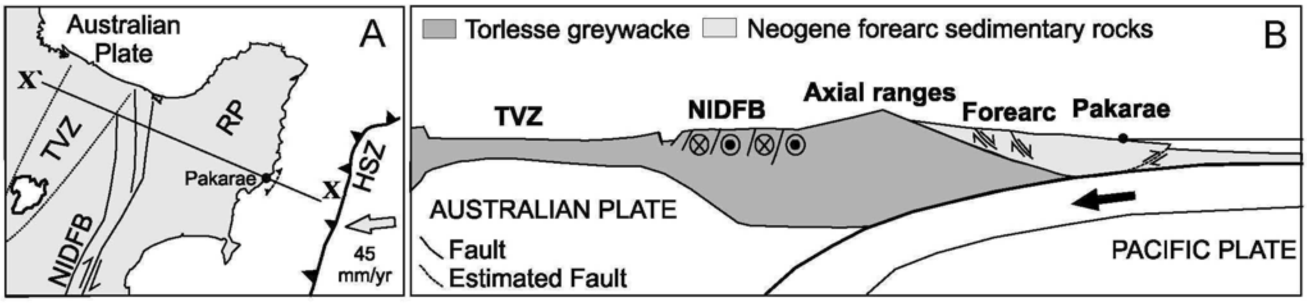

Fig. 7 **A**, Major tectonic elements of the Raukumara Peninsula sector of the Hikurangi margin. **B**, Schematic cross-section of the Raukumara Peninsula sector of the Hikurangi margin (X–X′) showing major upper plate structures and estimated location of a reverse fault offshore of the Pakarae River mouth. RP, Raukumara Peninsula; TVZ, Taupo Volcanic Zone; NIDFB, North Island Dextral Fault Belt; HSZ, Hikurangi Subduction Zone.

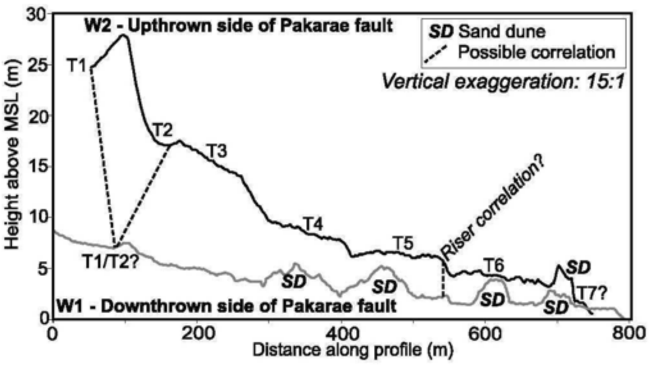

Fig. 8 Comparison of the topographic profiles on the downthrown (W1) and upthrown (W2) sides of the Pakarae Fault with possible correlation points.

with the uplift of the terraces. Correlation of terraces directly across the Pakarae Fault and comparison of riser heights led Ota et al. (1991) to suggest that the Pakarae Fault moved during some terrace uplift events, but that slip on this fault was not the primary cause of the regional coastal uplift. On the downthrown side of the Pakarae Fault, our profile (W1, Fig. 2) does not show the "staircase topography" characteristic of the upthrown side of the fault; rather, it is characterised by gentle slopes and sharp sand dune ridges (Fig. 2). Based on these data we cannot reliably correlate any terraces across the fault (Fig. 8), and suggest there are presently insufficient data to establish a relationship between Pakarae Fault movement and terrace formation. The terraces display a westward tilt towards the Pakarae Fault of 0.19° (Fig. 4), which argues against significant involvement of the Pakarae Fault in terrace uplift, because terraces in the footwall would be expected to have a tilt away from the fault (an eastwards tilt). The regional nature of the coastal uplift signal is corroborated by the similarity in the age of the marine terraces at Puatai Beach and Waihau Bay, 9 and 15 km north of Pakarae (Ota et al. 1991). Together, these datasets imply a domal uplift pattern with a wavelength of uplift along the coast of >15 km, as is consistent with slip on a major offshore fault striking parallel to the coast and dipping to the WNW (Ota et al. 1991). A revision of the Puatai Beach and Waihau Bay Holocene marine terraces and an evaluation of landward tilting on the Pakarae River fluvio-tectonic terraces are currently being prepared with the aim of refining the geometry of a probable causative offshore fault (Litchfield et al. "Coseismic fluvial terraces: an eample from the lower Pakarae River valley, Hikurangi margin, New Zealand" in prep.).

We use a simple schematic block model with an offshore reverse fault striking parallel with the coastline and an onshore normal fault striking perpendicular to the coastline to assess the likely structures driving coastal uplift (Fig. 9). Flexural isostasy dictates that the majority of absolute movement during slip on normal faults occurs through subsidence of the hanging wall (e.g., Jackson et al. 1988). Under various combinations of fault movement our model shows that the Pakarae geomorphology is most compatible with an offshore fault as the primary driver of coastal uplift (Fig. 9), in agreement with the conclusions of Ota et al. (1991).

Slip on a northwest-dipping offshore reverse fault would uplift both sides of the Pakarae Fault (Fig. 9A/1). Any synchronous or subsequent slip on the Pakarae Fault might be anticipated to cause subsidence of the downthrown block relative to MSL but not necessarily any significant vertical movement of the upthrown block relative to MSL (Fig. 9A/2). Vertical slip on the Pakarae Fault, in particular subsidence of its downthrown block, must have been less than the regional uplift related to slip on the offshore reverse fault, or else the western side of the fault would have been drowned due to net subsidence there, or be a flat coastal plain if coastal sedimentation rates were high enough to infill the embayment created by such net subsidence (Fig. 9B). To produce a terrace flight geomorphology similar to that of Pakarae with a downthrown block raised above MSL, these models show that the coastal uplift rate related to slip on the offshore fault must have been greater than the dip-slip rate of the Pakarae Fault (Fig. 9). The landward tilt of the terraces is compatible with back-tilt on an offshore coast-parallel reverse fault (Fig. 4).

The presence of an active reverse fault offshore of the Pakarae River mouth has important geodynamic implications for this sector of the Hikurangi margin. Presently only active normal faults have been mapped on the onshore Raukumara Peninsula (Mazengarb 1984, 1998; Mazengarb & Speden 2000), and geodetic studies show the region is currently undergoing extension and eastward rotation (Walcott 1987; Darby & Meertens 1995; Arnadottir et al. 1999; Wallace et al. 2004). The proposed offshore reverse fault is the first active contractional structure identified in a traverse from the

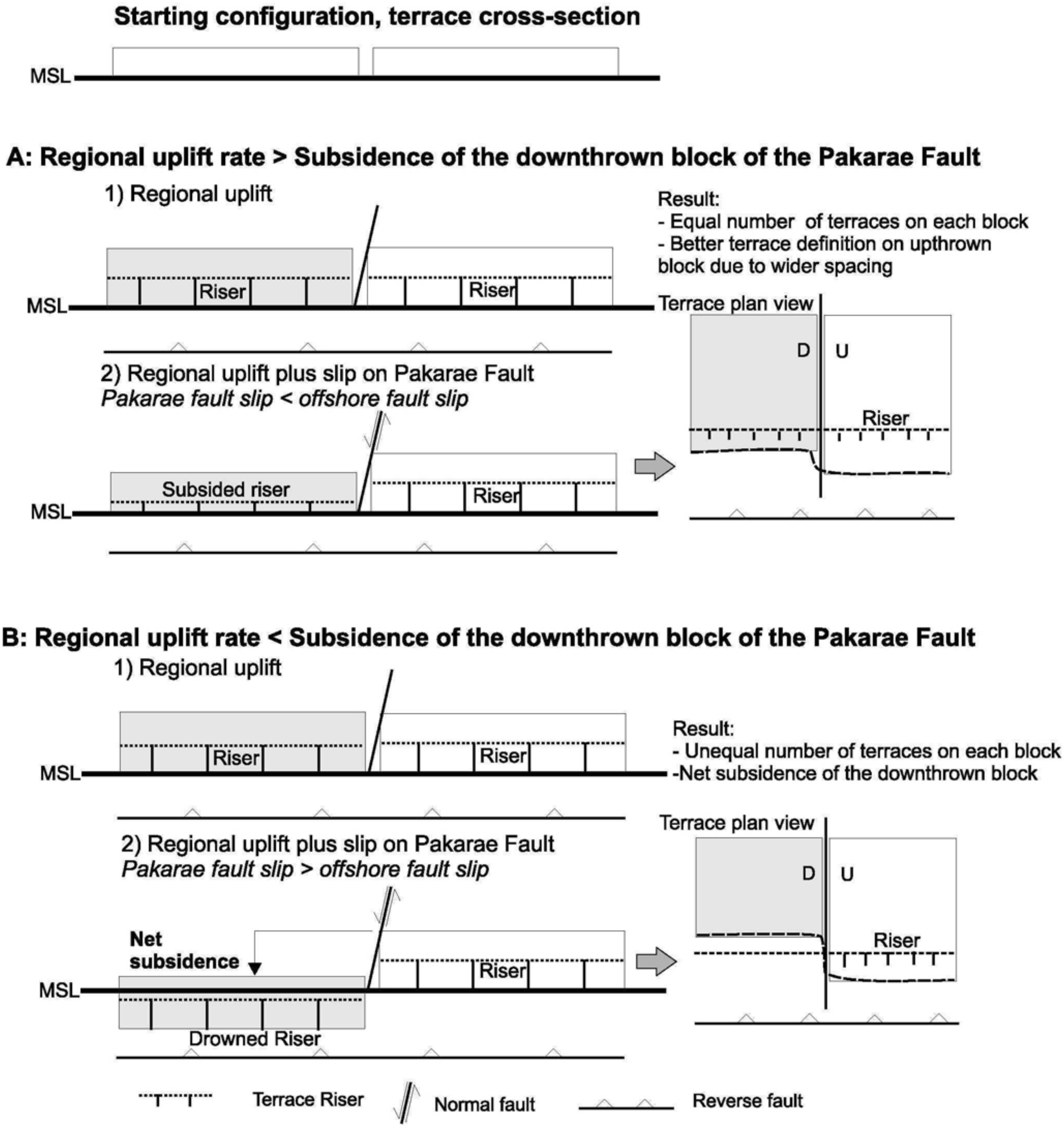

Fig. 9 Block models of an offshore reverse fault parallel with the marine terraces causing regional uplift, and a normal fault onshore perpendicular with the marine terraces. Two combinations of slip are shown, either regional uplift caused by the offshore fault is greater than dip-slip on the normal fault (A) or less than dip-slip on the normal fault (B). MSL = mean sea level.

backarc region to the Hikurangi Subduction Zone (Fig. 7B). Incorporation of offshore reverse faults in future studies of the Raukumara Peninsula is important; for example, examining whether such faults are listric to the plate interface, whether they interact with the interseismically locked portion of the interface, considering if reverse faults may accommodate a portion of the normal plate convergence motion along this segment of the margin, and incorporating faults on the continental shelf into tsunami hazard models of the region.

CONCLUSIONS

Our revision of the marine terrace distribution and chronology at Pakarae has shown that terrace formation and preservation either side of the Pakarae River is more uniform than previously described. Similar to Ota et al. (1991), we map seven terraces in total from T1 (representing the maximum Holocene transgression, and present only on the west bank) to T7 (the youngest terrace, preserved only on the east bank).

Terraces T2 through T6 are present on both sides of the river, although T3 is indistinct on the west bank and T5 is indistinct on the east bank. New age data from the east bank indicates that T2 is c. 4300 cal. yr BP, c. 2000 yr younger than the age of 6314–6195 cal. yr BP assigned by Ota et al. (1991). Terrace uplift has been intermittent. Average time intervals between uplift events range from 1280 to 630 yr and incremental uplift ranges from 2 to 4 m. Average Holocene uplift rates at Pakarae are relatively uniform over the past 7000 yr with a long term uplift rate of 3.2 ± 0.8 mm/yr.

Our study of the terrace geomorphology illustrates the importance of using the wave-cut strath elevation for terrace correlation rather than relying upon surface morphology, which is subject to a range of post-formation changes, especially in the development of coverbeds. It also demonstrates how multiple ages from the same terrace are preferable because shells from the same terrace used for radiocarbon dating can give variable results and have probably, in part, been reworked from older terraces. Future work is needed at this site to refine the terrace chronology, particularly of T7, which is not yet satisfactorily dated. Knowing the time of the most recent earthquake is important because the elapsed time since the last coastal uplift event may be critical to assessing the current seismic hazard at this location. To evaluate the tectonic structure chiefly responsible for terrace formation we need to reliably correlate the terraces across the Pakarae Fault and identify an offshore structure using marine geophysics. Block models indicate an offshore fault drives most or all of the coastal uplift, with synchronous or alternating smaller events on the Pakarae Fault causing relative subsidence of the western block of this normal fault.

ACKNOWLEDGMENTS

This research was funded by an EQC Student Grant (Project 6UNI/501). KJW is supported by the GNS-funded Sarah Beanland Memorial Scholarship. Rodger Sparks and Dawn Chambers of the Rafter Radiocarbon Laboratory are thanked for their contribution to the radiocarbon dating. Reviews by Yoko Ota, Harvey Kelsey, Philip Barnes, and an anonymous reviewer substantially improved this manuscript.

REFERENCES

Arnadottir T, Thornley S, Pollitz F, Darby DJ 1999. Spatial and temporal strain rate variations at the northern Hikurangi margin, New Zealand. Journal of Geophysical Research 104(B3): 4931–4944.

Barnes PM, Nicol A, Harrison T 2002. Late Cenozoic evolution and earthquake potential of an active listric thrust complex above the Hikurangi subduction zone, New Zealand. Geological Society of America Bulletin 114(11): 1379–1405.

Berryman KR 1993. Age, height, and deformation of Holocene terraces at Mahia Peninsula, Hikurangi subduction margin, New Zealand. 1. Tectonics 12(6): 1347–1364.

Berryman KR, Ota Y, Hull AG 1989. Holocene paleoseismicity in the fold and thrust belt of the Hikurangi subduction zone, eastern North Island, New Zealand. Tectonophysics 163: 185–195.

Berryman KR, Ota Y, Hull AG 1992. Holocene coastal evolution under the influence of episodoc tectonic uplift: examples from New Zealand and Japan. Quaternary International 15/16: 31–45.

Collot J-Y, Delteil J, Lewis K, Davy B, Lamarche G, Andru J-C, Barnes P, Chanier F, Chaumillon E, Lallemand S and others 1996. From oblique subduction to intra-continental transpression: structures of the southern Kermadec-Hikurangi margin from multibeam bathymetry, side-scan sonar and seismic reflection. Marine Geophysical Researches 18(2–4): 357–381.

Darby DJ, Meertens CM 1995. Terrestrial and GPS measurements across the Taupo backarc and Hikurangi forearc in New Zealand. Journal of Geophysical Research 100(B5): 8221–8232.

De Mets C, Gordon RG, Argus DF, Stein S 1994. Effect of recent revisions to the geomagnetic reversal timescale on estimates of current plate motions. Geophysical Research Letters 21: 2191–2194.

Froggatt PC, Lowe DJ 1990. A review of late Quaternary silicic and some other tephra formations from New Zealand: their stratigraphy, nomenclature, distribution, volume and age. New Zealand Journal of Geology and Geophysics 33: 89–109.

Gibb JG 1986. A New Zealand regional Holocene eustatic sea-level curve and its application to determination of vertical tectonic movements. A contribution to IGCP-Project 200. In: Reilly WI, Harford BE ed. Recent crustal movements of the Pacific region. Royal Society of New Zealand Bulletin 24: 377–395.

Hughen KA, Baillie MGL, Bard E, Beck JW, Bertrand CJH, Blackwell PG, Buck CE, Burr GS, Cutler KB, Damon PE, Edwards RL and others 2004. Marine04 Marine Radiocarbon Age Calibration, 0–26 cal kyr BP. Radiocarbon 46(3): 1059–1086.

Jackson JA, White NJ, Garfunkel Z, Anderson H 1988. Relations between normal-fault geometry, tilting and vertical motions in extensional terrains: an example from the southern Gulf of Suez. Journal of Structural Geology 10(2): 155–170.

Kingma JT 1964. Sheet 9—Gisborne. Geological map of New Zealand 1:250 000. Wellington, New Zealand, Department of Scientific and Industrial Research.

Lewis KB, Collot J-Y, Davy B, Delteil J, Lallemand S, Uruski C 1997. North Hikurangi GeodyNZ swath maps: depths, texture and geological interpretation 1:500 000. National Institute for Water and Atmospheric Research Miscellaneous Series Chart 72. Wellington.

Litchfield N, Wilson K 2005. Holocene tectonic fluvial terraces at Pakarae River mouth, Gisborne region. Programme and Abstracts, Geological Society of New Zealand 50th Annual Conference, Kaikoura New Zealand. Geological Society of New Zealand Miscellaneous Publication 119A: 45–46.

McFadgen BG 1985. Late Holocene stratigraphy of coastal deposits between Auckland and Dunedin, New Zealand. Journal of the Royal Society of New Zealand 15: 27–65.

Marsden ID 2004. Effects of reduced salinity and seston availability on growth of the New Zealand little-neck clam *Austrovenus stutchburyi*. Marine Ecology Progress Series 266: 157–171.

Marsden ID, Pilkington R 1995. Spatial and temporal variations in the condition of *Austrovenus stutchburyi* Finlay, 1927 (Bivalvia: Veneridae) from the Avon-Heathcote estuary, Christchurch. New Zealand Natural Sciences 22: 57–67.

Mazengarb C 1984. The Fernside Fault: an active normal fault, Raukumara Peninsula, New Zealand. New Zealand Geological Survey Record 3: 98–103.

Mazengarb C 1998. Late Neogene structural development of eastern Raukumara Peninsula: implications for oil exploration. 1998 New Zealand Petroleum Conference Proceedings: 201–205.

Mazengarb C, Speden IG comp. 2000. Geology of the Raukumara area. Institute of Geological & Nuclear Sciences 1:250 000 Geological Map 6. Lower Hutt, New Zealand, Institute of Geological & Nuclear Sciences Limited.

Morton J 2004. Seashore ecology of New Zealand and the Pacific. In: Hayward BW ed. Auckland, Bateman.

Morton J, Miller M 1968. The New Zealand sea shore. London, Collins.

Ota Y, Yamaguchi M 2004. Holocene coastal uplift in the western Pacific Rim in the context of late Quaternary uplift. Quaternary International 120: 105–117.

Ota Y, Berryman KR, Hull AG, Miyauchi T, Iso N 1988. Age and height distribution of Holocene transgressive deposits in eastern North Island, New Zealand. Palaeogeography, Palaeoclimatology, Palaeoecology 68: 135–151.

Ota Y, Hull AG, Berryman KR 1991. Coseismic uplift of Holocene marine terraces in the Pakarae River area, eastern North Island, New Zealand. Quaternary Research 35: 331–346.

Ota Y, Hull AG, Iso N, Ikeda Y, Moriya I, Yoshikawa T 1992. Holocene marine terraces on the northeast coast of North Island, New Zealand, and their tectonic significance. New Zealand Journal of Geology and Geophysics 35: 273–288.

Shane P, Froggatt PC, Smith I, Gregory M 1998. Multiple sources for sea-rafted Loisels Pumice, New Zealand. Quaternary Research 49: 271–279.

Stuiver M, Polach HA 1977. Discussion; reporting of C-14 data. Radiocarbon 19(3): 355–363.

Thornley S 1996. Neogene tectonics of Raukumara Peninsula, northern Hikurangi margin, New Zealand. Unpublished PhD thesis, Victoria University of Wellington, New Zealand.

Vucetich CG, Pullar WA 1964. Stratigraphy of Holocene ash in the Rotorua and Gisborne districts. Part 2. New Zealand Geological Survey Bulletin 73: 43–63.

Walcott RI 1987. Geodetic strain and the deformation history of the North Island, of New Zealand during the late Cainozoic. Philosophical Transactions of the Royal Society of London A321: 163–181.

Wallace LM, Beavan J, McCaffrey R, Darby D 2004. Subduction zone coupling and tectonic block rotations in the North Island, New Zealand. Journal of Geophysical Research 109(B12406): doi:10.1029/2004JB003241.

Wilson KJ, Berryman KB, Cochran UA, Little TA, in press. A Holocene incised valley infill sequence developed on a tectonically active coast: Pakarae River, New Zealand. Sedimentary Geology.

Yoshikawa T 1988. Pattern and rate of tectonic movement and late Quaternary geomorphic development in the Raukumara Peninsula, northeastern North Island, New Zealand. Bulletin of the Department of Geography University of Tokyo 20: 1–28.